

ADAPTIVE WAVELET TECHNIQUES FOR COMPRESSING DIGITAL MAMMOGRAMS

ALFRED BRUCKMANN, HARALD FLATSCHER,
THOMAS SCHELL AND ANDREAS UHL

*RIST++ & Department of Scientific Computing,
University of Salzburg,
Hellbrunnerstr. 34, 5020 Salzburg, Austria
{abruck, hflatsch, tschell, uhl}@cosy.sbg.ac.at*

Abstract: In this work we investigate the possible benefit of employing adaptive wavelet algorithms instead of the classical fixed pyramidal wavelet decomposition for the compression of digital mammograms. In particular, we target on adaptive wavelet packet and NSMRA decompositions. We observe that information cost function optimized wavelet packet subband structures do not offer compression performance gain in this case whereas NSMRA decompositions moderately improve the results of classical wavelet decompositions. Due to the lack of fast and reliable search algorithms fixed NSMRA decompositions need to be generated and employed for classes of similar images.

Keywords: wavelet compression, wavelet packets, time-varying decomposition, NSMRA, mammograms

1. Introduction

Wavelet-based image processing methods have gained much attention in the biomedical imaging community. Applications range from pure biomedical image processing techniques such as noise reduction, image enhancement, and detection of microcalcifications in mammograms to computed tomography (CT) magnetic resonance imaging (MRI), and functional image analysis (positron emission tomography (PET) and functional MRI) [44, 1].

Image compression methods that use wavelet transforms [40] which are based on multiresolution analysis — (MRA) have been successful in providing high rates of compression while maintaining good image quality, and have proven to be serious competitors to discrete cosine transform — (DCT) [47, 33] or fractal — [16, 17, 27] based compression schemes. A wide variety of wavelet-based image compression schemes have been reported in the literature [3, 20, 26], ranging from simple entropy coding to more complex techniques such as vector quantization [2, 12], adaptive transforms [14, 41], zero-tree encoding [37], and edge-based coding [18]. The

latest compression algorithms are based on set partitioning in hierarchical trees [35] and some improvements in arithmetic coding [51]. In several papers (see e.g. [4, 32, 15]) the suitability of different lossy compression schemes with respect to medical images have been investigated thoroughly. In accordance to the results for general image types it has been found that advanced wavelet based compression schemes offer the best rate–distortion performance of all coders considered. Also aspects of lossless wavelet–based compression of medical images [45], as well as techniques for wavelet–based compression of medical video data [21, 48], have been described in the literature.

Medical image compression is constrained by the fact that most radiologists are not willing to base a diagnosis on an image that has been compressed in a lossy way. This is partially due to legal reasons (depending on the corresponding country’s laws) and partially due to the fear of misdiagnosis because of lost data in the compression procedure [50]. Therefore, only lossless and visually lossless techniques are accepted. On the other hand, many medical professionals are convinced that the future of health care will be shaped by technologies such as telemedicine. Applications of this type demand lower data rates as are achievable with most currently used schemes [11]. Consequently, highly efficient and widely accepted techniques for medical image compression are needed.

In this paper we investigate the possible benefit of employing adaptive wavelet algorithms instead of the classical fixed pyramidal wavelet decomposition. The idea of using adaptive algorithms can be used in two ways: on the one hand, the adaptive process can be performed for each new image thereby causing computational and coding overhead as compared to the non–adaptive case, on the other hand the same (adaptively generated) setting may be employed for classes of similar images (this has been done in the context of the FBI fingerprint compression standard [22]). In particular, we target here onto the transform step of the wavelet compression scheme and investigate adaptively generated subband structures (“wavelet packets”) and time–variant filterbanks (“NSMRA decomposition”) with respect to their performance in compressing mammograms.

2. Wavelet Packet Compression

2.1 Wavelet Packet Decomposition and Basis Choice

Wavelet packets [49] represent a generalization of the method of multiresolution decomposition and comprise the entire family of subband coded (tree) decompositions. Whereas in the wavelet case the decomposition is applied recursively to the coarse scale approximations only (leading to the well known (pyramidal) wavelet decomposition tree), in the wavelet packet (WP) decomposition the recursive procedure is applied to all the coarse scale approximations and detail signals, which leads to a complete WP tree (i.e. binary tree and quadtree in the 1D and 2D case, respectively see Figure 1) and more flexibility in frequency resolution.

There are several possibilities how to determine the frequency subbands suited well for an application (the meaning of *suitable* depends on the type of application,

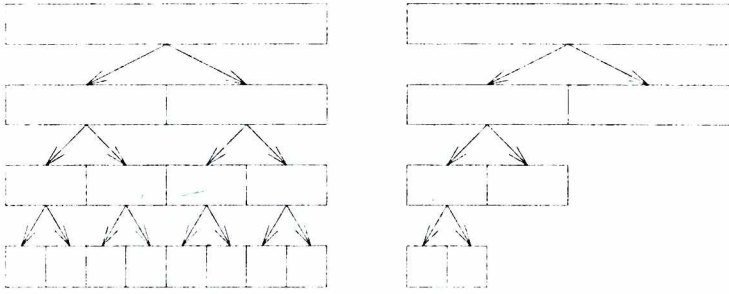


Figure 1. 1D wavelet packet and pyramidal wavelet decomposition tree

e.g. signal/image compression [49], feature extraction [36], classification algorithms [23, 24], telecommunication applications [25], numerical mathematics [31], and many more). The WP “best basis algorithm” [10] performs an adaptive optimization of the frequency resolution of a complete WP decomposition tree by selecting the most suitable frequency subbands for signal compression. This is done by optimizing additive information cost functions. The same algorithm employed with non-additive cost function is denoted “near-best basis algorithm” [39], if the subband structure is restricted to uniform time–frequency resolution the corresponding algorithm is denoted “best level selection” [49].

In the context of image compression a more advanced technique is to use a framework that includes both rate and distortion, where the best basis subtree which minimizes the global distortion for a given coding budget is searched [34]. Other methods use fixed bases of subbands for similar signals (e.g. fingerprints [22]) or search for good representations with a genetic algorithm [6, 5]. Recently, WP based compression methods have been developed [52, 30] which outperform the most advanced wavelet coders (e.g. SPIHT [35]) significantly for textured images in terms of rate–distortion performance.

However, the class of images for which excellent results have been achieved with wavelet packet methods is somewhat limited. Usually, special frequency characteristics are required to guarantee a better behaviour as compared to the wavelet case: this has been shown for fingerprints [22] (and was verified with our software as well [5] in that case) and for the testimage “Barbara” [29, 52, 30]. Here, we will investigate whether mammograms exhibit similar features to make wavelet packet techniques profitable. Additionally, newly developed non-additive cost functions for the near best basis algorithm are evaluated within that application framework. Classical non-additive information cost functions (as given in [39]) include the (non-additive) Shannon entropy, the weak l^p -norm, and the data compression area. Our search for new cost functions has two motivations:

1. good cost function values do not necessarily imply good rate/distortion performance so far;
2. the evaluation of most cost functions mentioned above causes high computational demand due to the sorting algorithms involved.

Let (x_1, x_2, \dots, x_n) be a sequence of transform coefficients. We introduce the following non-additive cost function:

Concentration: The interval containing the transform coefficients $([\min_{1 \leq i \leq n}(x_i), \max_{1 \leq i \leq n}(x_i)])$ is partitioned into q equal-sized intervals $[a_j, a_{j+1}]$ with $a_0 = \min_{1 \leq i \leq n}(x_i)$ and $a_q = \max_{1 \leq i \leq n}(x_i)$. We set $H_j = \#(x_i \in [a_{j-1}, a_j])$, $h_j = H_j/n$, and $k_j = \sum_{i=1}^j h_i$ for $j = 1, \dots, q$, $k_0 = 0$. The Lorenz measure of concentration (LMC) (also denoted Gini-coefficient [19]) is defined as:

$$LMC = \sum_{j=1}^q (k_{j-1} + k_j) \frac{a_j H_j}{\sum_{i=1}^q a_i H_i} - 1.$$

LMC holds $0 \leq LMC \leq (n-1)/n$ and originates from measures of concentration for frequency distributions. The higher the value of concentration the better suited for compression is the sequence of coefficients.

2.2 Experiments

In our experiments we use a set of mammograms with 256 graylevels (8 bpp) and 256×256 pixels size, results are given for one representative only (see Figure 2a) since the other results are comparable. We use the so-called ‘‘Dartmouth Wavelet Tool Box’’ codec developed by G. Davis which is available for free for research purposes at <http://www.cs.dartmouth.edu/~gdavis/wavelet/wavelet.html> in order to allow a high degree of comparability of our results. The software is used with Daubechies’ compactly-supported wavelets [13] with 10 filter taps and 5 levels of decomposition with periodic border padding. We have used the corresponding family of filters successfully in previous work [41, 43], see Villasenor [46] for a discussion about proper filter choice for wavelet coding. The multilayer, embedded quantizer with arithmetic coder is employed. In order to adapt this software to the requirements of wavelet packet coefficient coding, we use the frequency oriented scan-ordering proposed in [30].

The compression ratio is defined as:

$$\frac{\text{number of bits in the original image}}{\text{number of bits in the compressed image}}.$$

Peak signal-to-noise ratio (PSNR) is used as an objective measure of image quality and is defined as follows (measured in deciBel dB):

$$PSNR = 10 \log_{10} \frac{225^2}{e_{ms}^2},$$

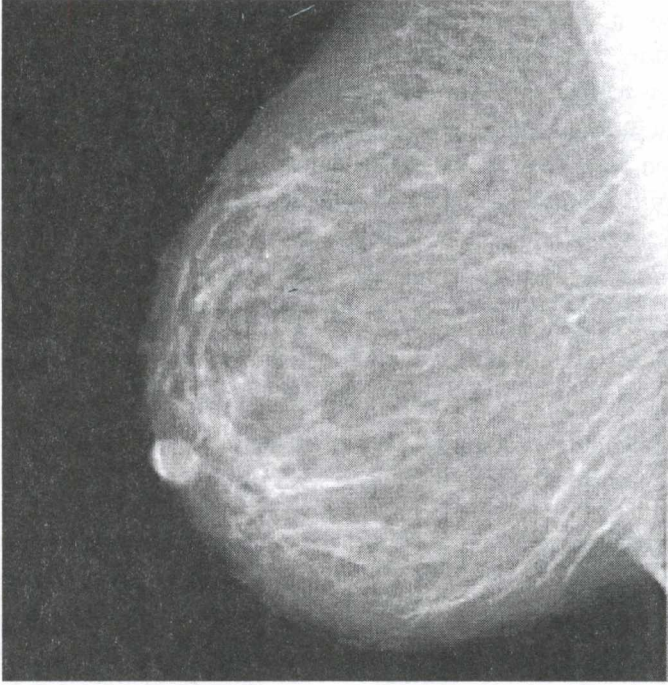
where 255 is the maximal gray-value of the original image and e_{ms}^2 is the average sample mean-squared error:

$$e_{ms}^2 = \frac{1}{N^2} \sum_{i=1}^N \sum_{j=1}^N (f(i, j) - \hat{f}(i, j))^2,$$

where $f(i, j)$ and $\hat{f}(i, j)$ represent the $N \times N$ original and the reproduced images, respectively.

In Figure 2b we see a typical result for mammograms (and as well typical for

a)



b)

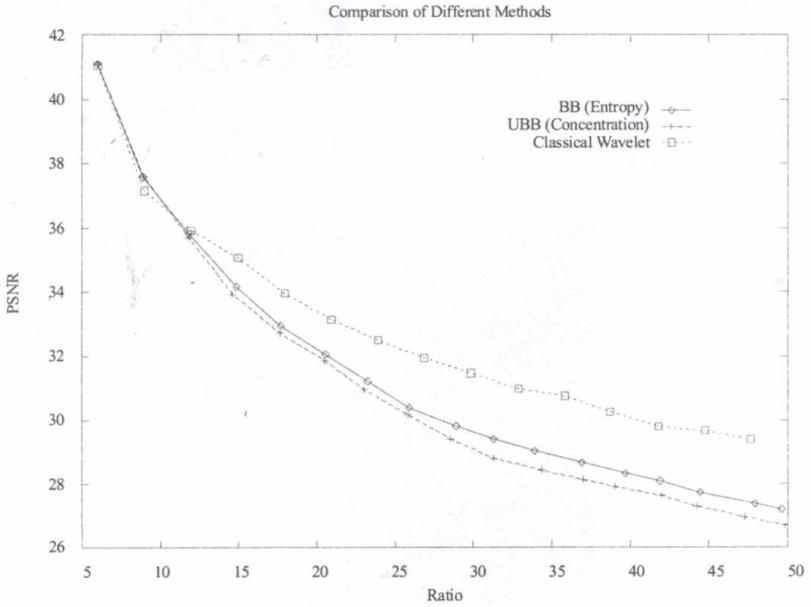


Figure 2. Adaptive vs non-adaptive compression of a mammogram: a) mammogram, b) compression performance

several tested angiograms): The classical wavelet approach significantly outperforms both adaptive algorithms in terms of rate–distortion performance (up to 20 dB more). Additionally, the classical best basis algorithm employing additive entropy as cost function is slightly better than the near best basis approach using concentration as cost function (although this cost function has proven to give good rate–distortion performance for fingerprints [5]). Figure 3 shows the corresponding subband structures as employed in the compression process (subbands at lower decomposition levels are displayed in darker gray). Obviously, the computational demand for the adaptively generated subband structures is higher as compared to the classical case (even if the structures are calculated once and subsequently used for similar images). Based on this and similar results for other mammograms we may summarize that for mammogram–type images the following may be stated:

- classical fixed wavelet decomposition is superior to cost–function optimized adaptive wavelet packet subband structures;
- sophisticated non additive cost–functions do not necessarily give better results than classical simple additive ones.

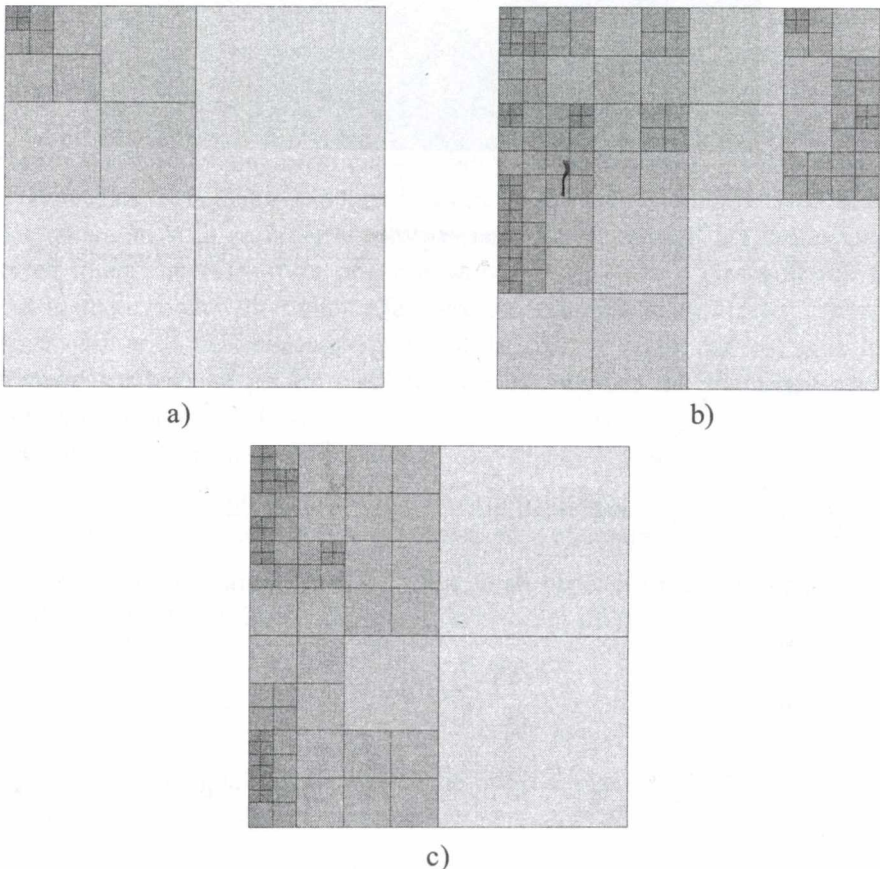


Figure 3. Subband structures for a mammogram: a) classical wavelet, b) NBB (Concentration), c) BB (Entropy)

In the following, we evaluate the rate–distortion performance of subband structures generated by optimizing the non–additive cost function “quadratic compression area” as proposed in [38, 39]. Figure 4a compares the cost function values of the subband structures corresponding to the classical wavelet decomposition and this generated by the near best basis algorithm (two horizontal lines) to the evolution of the values of subband structures in time optimized with a genetic algorithm (see [5, 6] for more details). Note that the cost function value in

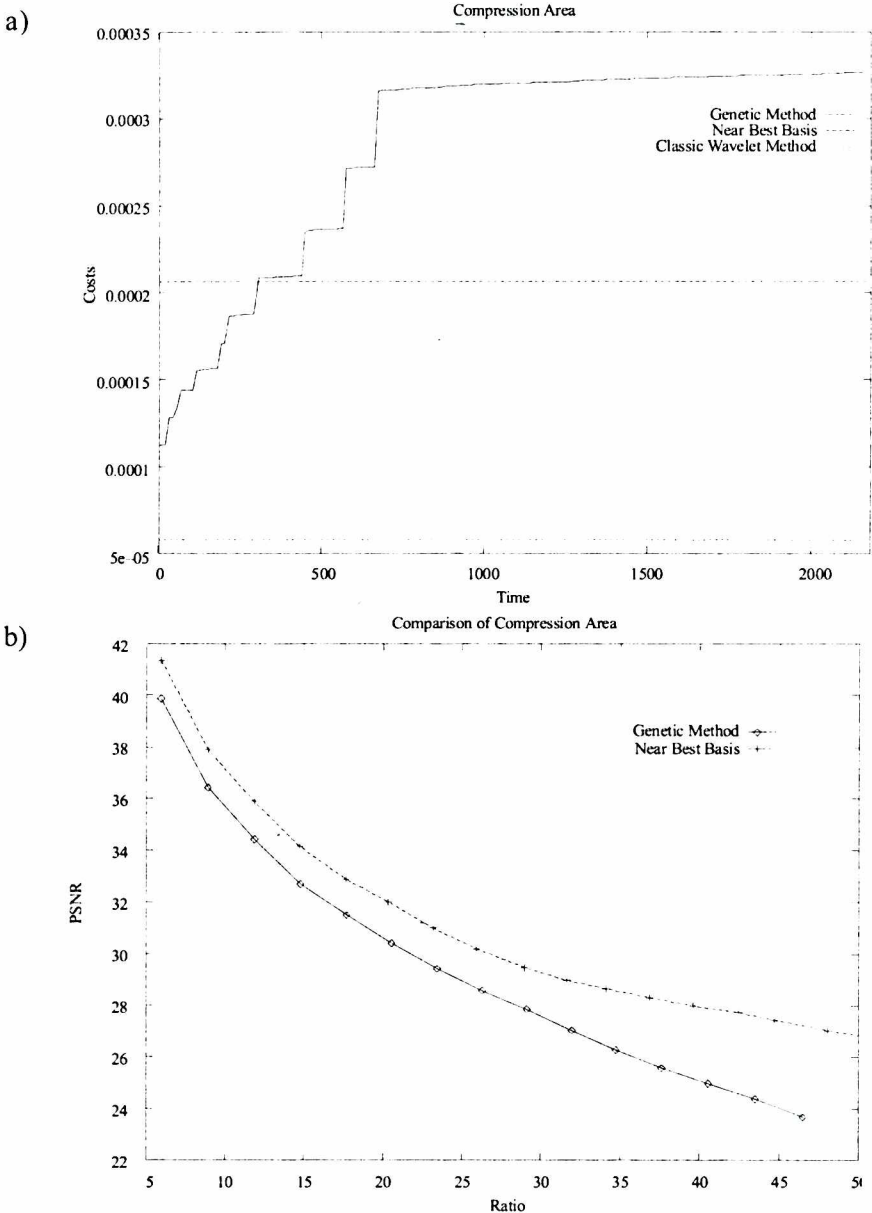


Figure 4. Behaviour of non–additive cost function “compression area”:
a) cost function evolution, b) compression performance

the plot corresponds to $1/(1+cost)$ due to internal reasons within the genetic algorithm implementation. As a matter of fact, the near best basis subband structure is superior to the pyramidal wavelet decomposition in terms of compression area. Obviously, the value achieved with the near best basis algorithm is far from being optimal since the genetic algorithm reaches much better values. Interestingly, these results are of minor relevance for the rate–distortion performance. Figure 4b reveals that the subband structure corresponding to the near best basis algorithm shows clearly better rate–distortion performance as compared to that corresponding to the genetic algorithm (which has better cost function values). This property also holds if we compare Figures 4b and 2b since again the classical wavelet method is superior. This obviously shows that within the set of subband structures with acceptable values in terms of compression area (which is fairly large) the ranking with respect to compression area has little to do with the ranking with respect to rate–distortion performance.

A second comparison of Figures 4b and 2b shows that the cost function concentration performs almost equally as the cost function compression area with respect to rate–distortion performance — this is achieved at a significantly lower computational cost for concentration. Additionally it is interesting to see that the subband structures corresponding to the two cost functions are fairly different (Figure 3b (concentration) vs 5a (compression area)) but lead to almost identical rate–distortion curves.

Summarizing we may clearly state that subband structures generated by the best basis or near best basis algorithm lead to worse rate–distortion performance as compared to classical wavelet decomposition for mammogram–type images. Therefore, their use for this specific application can not be recommended.

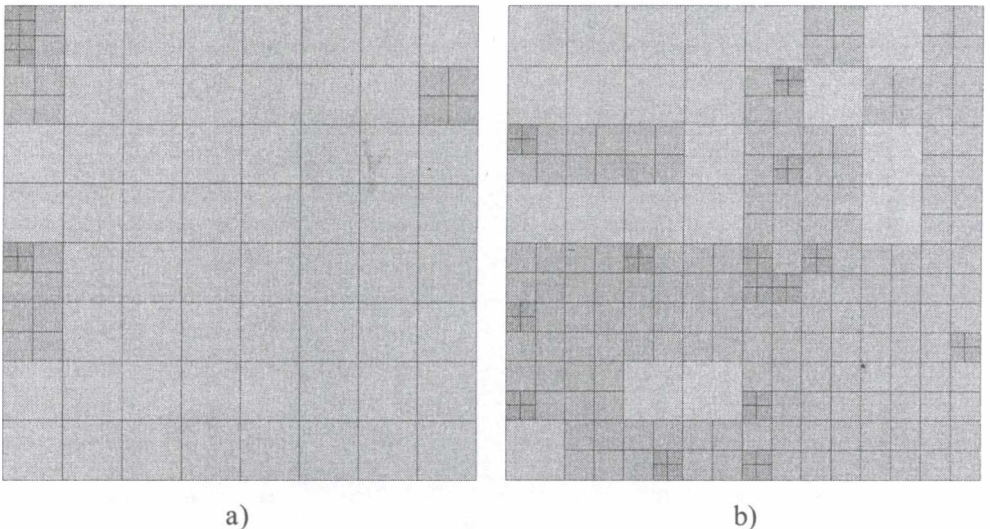


Figure 5. Subband structures corresponding to the cost function "compression area" using different optimization techniques: a) near best basis algorithm, b) genetic algorithm

3. NSMRA Compression

3.1 NSMRA Decomposition and Algorithms

In the classical MRA scheme one uses a set of well chosen filter coefficients to perform a convolution followed by a decimation from fine to coarse scales. Since all the transformations at each level are performed independently, it is possible to use different filter coefficients at every scale. This theory of non-stationary MRA (NSMRA) was introduced in [9]—based on this there have been some papers published on exploiting the freedom in choosing different wavelet filters for different scale levels for adaptive image coding techniques (e.g. using a filter library [42, 41, 43] and an adaptive filter design approach [14, 28]).

The classical 2-D wavelet decomposition is implemented by first convolving the rows of the low pass image S_{j+1} (or the original image in the first decomposition step) with the QMF filterpair G and H (which are a high pass and a low pass filter, respectively), retaining every other row, then convolving the columns of the resulting images with the same filterpair and retaining every other column. The same procedure is applied again to the coarse scale approximation S_j and to all subsequent approximations.

Since all the convolutions at different scale (or resolution) levels and image directions are performed independently we can define a generalized decomposition as follows:

A NSMRA wavelet decomposition is obtained by using different filterpairs for different scale levels of the decomposition (e.g. Figure 6: filterpair G, H at scale level $j + 1$, filterpair A, B at scale level j).

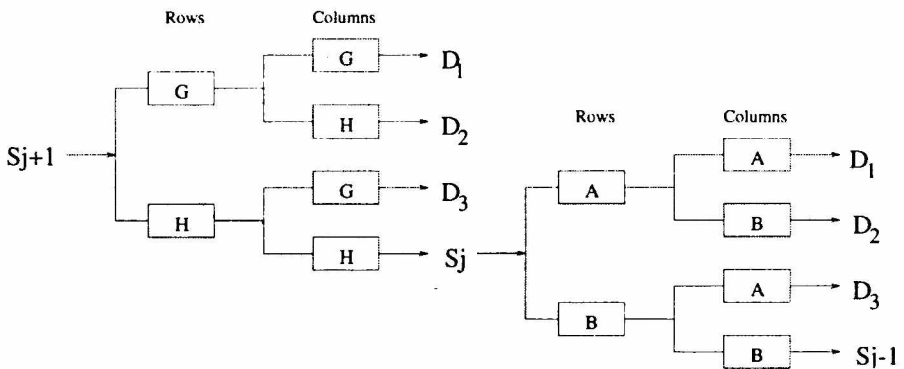


Figure 6. 2-D NSMRA wavelet decomposition

Suppose we have given a filter library containing l pairs of different wavelet filters and a fixed maximal decomposition depth m . It is possible to build with the filters contained in this library l^m different NSMRA wavelet decompositions (always including classical ones). Now we describe an algorithm that identifies good filter combinations in this big set of possible ones in terms of a tree search problem.

Beginning at the top of the tree, we expand for the first scale level into l branches (corresponding to the decompositions using the l different filterpairs) and get l children nodes. Each of these nodes is expanded again for the second scale level into l branches leading to l^2 nodes at the second scale level. When the whole tree is expanded we arrive at l^m nodes at the bottom of the tree which correspond to l^m possible NSMRA decompositions using a library and decomposition depth of the given order.

Finding the best NSMRA decomposition in this tree corresponds to finding the node at the bottom level that gives the lowest information cost. A NSMRA decomposition is represented by a path from the root to a bottom node in the tree.

A local optimization algorithm (also denoted “best level filter selection algorithm” in [41]) can be described in terms of searching in this NSMRA decomposition tree as follows. After the decomposition of the first scale level using all the l filterpairs only the node with the best cost function value (this may be an information cost function e.g. entropy (see last section) evaluated on the detail images only or any rate–distortion based cost function) is expanded into its l branches (corresponding to the second scale level). The resulting l nodes are again evaluated and only the best one is expanded. Following this procedure, only ml paths are investigated instead of l^m in a complete search.

In terms of classical tree search this local optimization algorithm is a hill–climb or a beam search expanding only the best node. Parallel algorithms for this type of search procedure have been already proposed [42].

3.2 Experiments

Our experiments have been confined to pyramidal subband structures and we may therefore employ a codec optimized for that setting. We use the so–called “SPIHT” codec [35] developed by A. Said and W. Pearlman which is available (source–code is no longer available) at <http://ipl.rpi.edu:80/SPIHT/> in a reduced version. As before, decomposition depth is fixed to $m = 5$. The filter library consists of Daubechies’ compactly–supported wavelets [13] ranging from 2 to 16 filter taps (consequently, $l = 8$) denoted d2–d16. The cost function employed is PSNR measured for each decomposition stage at specific compression ratios (in this case 10, 20 and 80). In Figure 7 we display results for the following algorithms:

- **MAX–Singlefilter:** The highest PSNR value achieved by classical decomposition with a filter contained in the library;
- **MIN–Singlefilter:** The lowest PSNR value achieved by classical decomposition with a filter contained in the library;
- **FULL_SEARCH:** The highest PSNR value achieved by exhaustive search through $l^m = 32768$ possible NSMRA decompositions;
- **LOCAL_OPTIMIZATION:** The PSNR value achieved by local optimization as described before.

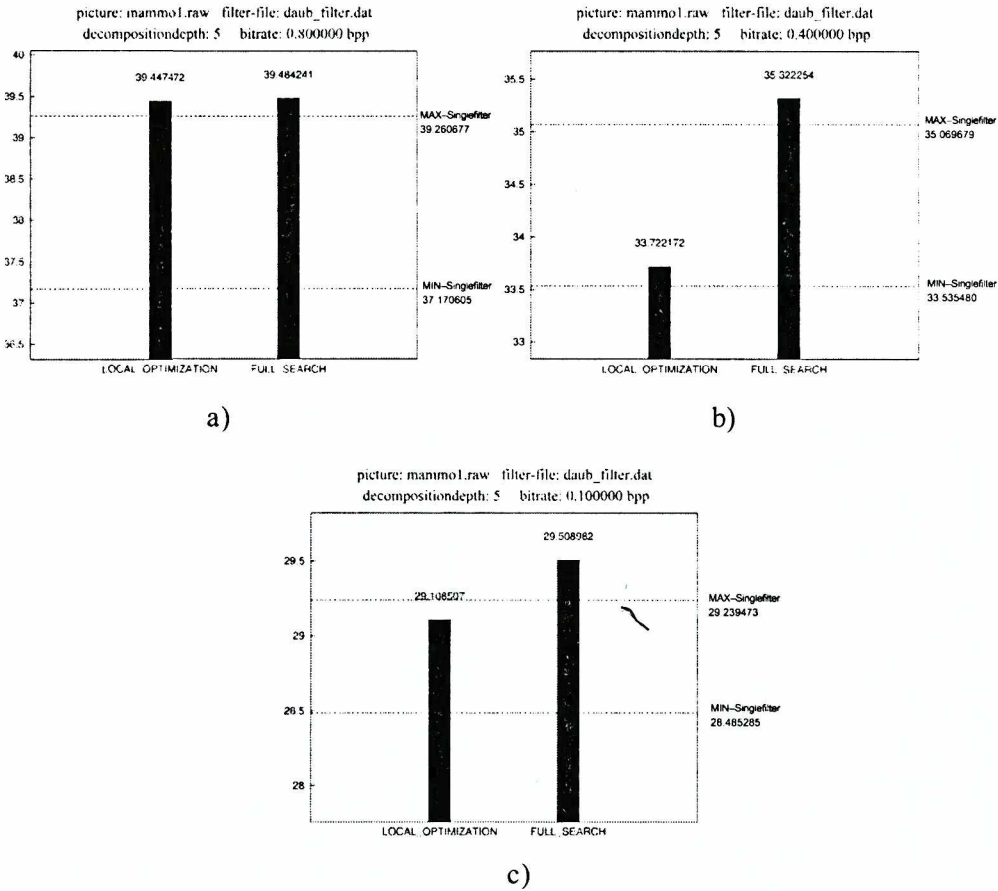


Figure 7. Results of NSMRA compression at various compression ratios: a) 10, b) 20, c) 80

Whereas the results of exhaustive NSMRA search are always better as compared to the best classical wavelet decomposition (about 0.22–0.26 dB) this holds for local optimization only in the case of compression ratio 10. Table 1 shows the filter combinations found by the different algorithms (where e.g. d(14,10,10,4,12) denotes a NSMRA decomposition with d14 at the first scale level, d10 at the second, and so on).

In the case of compression ratios 10 and 20 the choice of the filters seems to exhibit a regular pattern: For the classical decomposition, longer filters give the best results whereas d2 performs worst (this is a well known fact). The best NSMRA decompositions employ longer filters at high scale levels and shorter ones at lower decomposition levels, for the worst NSMRA decompositions it is exactly vice versa. However, local optimization only follows this scheme at compression ratio 10 and this is the only case where the results are competitive (in the other cases, local search is “trapped” by fixing d2 at high scale levels). On the other hand no regular pattern with respect to filter choice seems to be present at compression ratio 80.

Table 1. Decomposition schemes found with the different algorithms

<i>C-ratio</i>	<i>Max</i>	<i>Min</i>	<i>Local-NSMRA</i>	<i>Max-NSMRA</i>	<i>Min-NSMRA</i>
10	d12	d2	d(14,10,10,4,12)	d(14,10,6,2,2)	d(2,2,16,16,14)
20	d14	d2	d(2,14,12,6,8)	d(14,12,6,6,10)	d(2,2,16,16,10)
80	d4	d16	d(2,2,4,4,10)	d(14,10,10,8,10)	d(12,2,2,2,16)

Figure 8 displays reconstructed mammograms compressed at ratio 80 using the decomposition schemes “Max” and “Max-NSMRA” given in Table 1. It seems that in the NSMRA case less detail is lost and the artifacts are less pronounced.

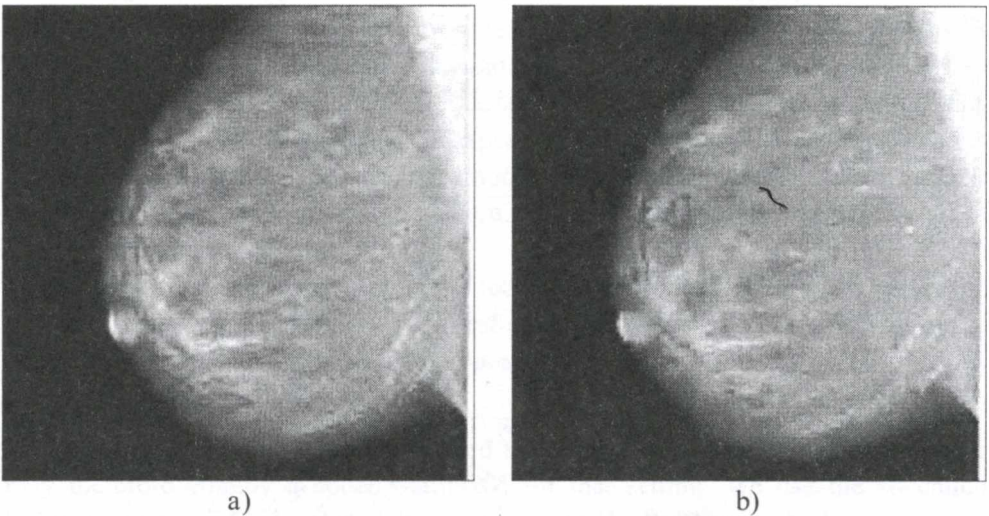


Figure 8. Comparison of NSMRA and wavelet compression at compression ratio 80:
a) NSMRA, b) wavelet

Summarizing, we have found that adaptive NSMRA decompositions may slightly improve the rate-distortion performance of classical wavelet codecs for mammogram-type images. However, the existing fast adaptation algorithms have proven to be not very reliable. Therefore, only the approach of training NSMRA decompositions with a class of representative images and subsequent fixing of the decomposition scheme seems promising.

4. Conclusion

In this work we have investigated the possible benefit of employing adaptive wavelet algorithms instead of the classical fixed pyramidal wavelet decomposition for the compression of digital mammograms. In particular, we target on adaptive wavelet packet and NSMRA decompositions. Although it is often claimed that information cost function optimized wavelet packets offer compression performance gain over classical wavelet decompositions we have found the contrary to be true in the case of mammogram-type images, whereas adaptive NSMRA decompositions

moderately improve the results of classical wavelet decompositions. Due to the lack of fast and reliable search algorithms it is not possible to perform the NSMRA adaptation process for each new image individually. Fixed NSMRA decompositions need to be generated by adaptation onto a training set and employed for classes of similar images.

Acknowledgements

The first three authors are partially supported by the Austrian Science Fund FWF, project no. P11045-ÖMA.

References

- [1] A. Aldroubi and M. Unser, editors. *Wavelets in Medicine and Biology*. CRC, Boca Raton, FL, USA, 1996
- [2] M. Antonini, M. Barlaud, P. Mathieu and I. Daubechies. Image coding using wavelet transform. *IEEE Transactions on Image Processing*, 1(2): 205–220, 1992
- [3] A. Averbuch, D. Lazar and M. Israeli. Image compression using wavelet transform and multiresolution decomposition. *IEEE Trans. on Image Process.*, 5(1): 4–15, 1996
- [4] K. Belloulata, A. M. Baskurt, H. Benoit-Cattin and R. Prost. Fractal coding of medical images. In Y. Kim, editor. *Medical Imaging 1996: Image Display*, volume 2707 of *SPIE Proceedings*, pages 598–609, Newport Beach, CA, USA, April 1996, *SPIE*
- [5] A. Bruckmann, Th. Schell and A. Uhl. Evolving subband structures for wavelet packet based image compression using genetic algorithms with non-additive cost functions. In *Proceedings of the International Conference "Wavelets and Multiscale Methods" (IWC'98), Tangier, 1998*. INRIA, Rocquencourt, April 1998, 4 pages
- [6] C. H. Chui. Genetic algorithm search of multiresolution tree with applications in data compression. In H. H. Szu, editor, *Wavelet Applications*, volume 2242 of *SPIE Proceedings*, pages 950–958, 1994
- [7] C. K. Chui, editor. *Wavelets: A Tutorial in Theory and Applications*. Academic Press, San Diego, 1992
- [8] C. K. Chui, L. Montefusco and L. Puccio. *Wavelets: Theory, Algorithms and Applications*. Academic Press, San Diego, 1994
- [9] A. Cohen. Non-stationary multiscale analysis. In [8], pages 3–12 Academic Press, 1994
- [10] R. R. Coifman and M. V. Wickerhauser. Entropy based methods for best basis selection. *IEEE Transactions on Information Theory*, 38(2): 719–746, 1992
- [11] P. C. Cosman, R. M. Gray and R. A. Olshen. Evaluating quality of compressed medical images: SNR, subjective rating and diagnostic accuracy. *Proceedings of the IEEE*, 82(6): 919–932, 1994
- [12] P. C. Cosman, R. M. Gray and M. Vetterli. Vector quantization of image subbands: A review. *IEEE Transactions on Image Processing*, 5(2): 202–205, 1996
- [13] I. Daubechies. Orthonormal bases of compactly supported wavelets. *Comm. Pure and Appl. Math.*, 41: 909–996, 1988
- [14] P. Desarte, B. Macq and D. T. M. Slock. Signal-adapted multiresolution transform for image coding. *IEEE Transactions on Information Theory*, 38(2): 879–904, 1992

- [15] B. J. Erickson, A. Manduca, P. Palisson, K. R. Persons, F. Earnest IV, V. Savchenko and N. J. Hangandreou. Wavelet compression of medical images. *Radiology*, 206(3): 599–607, 1998
- [16] Y. Fisher, editor. *Fractal Image Compression: Theory and Application*. Springer–Verlag, New York, 1995
- [17] Y. Fisher, editor. *Fractal Image Encoding and Analysis*, volume 195 of *NATO ASI Series. Series F: Computer and Systems Sciences*. Springer–Verlag, Berlin, Heidelberg, New York, Tokyo, 1998
- [18] J. Froment and S. Mallat. Second generation compact image coding. In [7], 655–678, Academic Press, 1992
- [19] J. Hartung, editor. *Statistik: Lehr– und Handbuch der angewandten Statistik*. Oldenbourg, München, Wien, 1995
- [20] M. L. Hilton, B. D. Jawerth and A. Sengupta. Compressing still and moving images with wavelets. *Multimedia Systems*, 3(2), 1995
- [21] B. K. T. Ho, M.–J. Tsai, J. Wei, M. Ma and P. Saipetch. Video compression of coronary angiograms based on discrete wavelet transform with block classification. *IEEE Transactions on Medical Imaging*, 15(6), December 1996
- [22] T. Hopper. Compression of gray–scale fingerprint images. In H. H. Szu, editor, *Wavelet Applications*, volume 2242 of *SPIE Proceedings*, pages 180–187, 1994
- [23] A. Laine and J. Fan. Texture classification by wavelet packet signatures. *IEEE Transactions on Pattern Analysis and Machine Intelligence*, 11(15): 1186–1191, 1993
- [24] R. E. Learned and A. S. Willsky. A wavelet packet approach to transient signal classification. *Applied and Computational Harmonic Analysis*, 2: 265–278, 1995
- [25] A. R. Lindsey and J. C. Dill. Digital transceiver implementation for wavelet packet modulation. In H. H. Szu, editor, *Wavelet Applications V*, volume 3391 of *SPIE Proceedings*, pages 255–264, SPIE, 1998
- [26] J. Lu, V. R. Algazi and R. R. Estes. Comparative study of wavelet image coders. *Optical Engineering*, 35(9): 2605–2619, 1996
- [27] N. Lu, editor. *Fractal Imaging*. Academic Press, San Diego, CA, 1997
- [28] B. Macq and J. Y. Mertens. Optimization of linear multiresolution transforms for scene adaptive coding. *IEEE Trans. on Signal Process.*, 41(12): 3568–3572, 1993
- [29] D. Marpe, H. L. Cycon and W. Li. Complexity constrained best–basis wavelet packet algorithm for image compression. *IEEE Proceedings Vision, Image and Signal Processing*, 145(6): 391–398, 1998
- [30] F. G. Meyer, A. Z. Averbuch, J. O. Strömberg and R. R. Coifman. Fast wavelet packet image compression. In *Proceedings of the Data Compression Conference DCC'98*, page 563, IEEE Press, March 1998
- [31] L. Bacchelli Montefusco. Semi–orthogonal wavelet packet bases for parallel least–squares approximation. *Journal of Computational and Applied Mathematics*, 73: 191–208, 1996
- [32] L. P. Panych. Theoretical comparison of Fourier and Wavelet encoding in Magnetic Resonance Imaging. *IEEE Trans. on Medical Imaging*, 15(2): 141–153, 1997
- [33] W. B. Pennebaker and J. L. Mitchell. *JPEG Still — image compression standard*. Van Nostrand Reinhold, 1993
- [34] K. Ramchandran and M. Vetterli. Best wavelet packet bases in a rate–distortion sense. *IEEE Trans. on Image Process.*, 2(2): 160–175, 1993

- [35] A. Said and W. A. Pearlman. A new, fast and efficient image codec based on set partitioning in hierarchical trees. *IEEE Transactions on Circuits and Systems for Video Technology*, 6(3): 243–249, 1996
- [36] N. Saito and R. R. Coifman. Local discriminant bases. In A. F. Laine and M. A. Unser, editors, *Wavelet Applications in Signal and Image Processing II*, volume 2303 of *SPIE Proceedings*, pages 2–14, 1994
- [37] J. M. Shapiro. Embedded image coding using zerotrees of wavelet coefficients. *IEEE Trans. on Signal Process.*, 41(12): 3445–3462, 1993
- [38] C. Taswell. Near–best basis selection algorithms with non–additive information cost functions. In Moeness Amin, editor, *Proceedings of the IEEE International Symposium on Time–Frequency and Time–Scale Analysis*, pages 13–16, IEEE Press, 1994
- [39] C. Taswell. Satisficing search algorithms for selecting near–best bases in adaptive tree–structured wavelet transforms. *IEEE Transactions on Signal Processing*, 44(10): 2423–2438, 1996
- [40] P. N. Topiwala, editor. *Wavelet Image and Video Compression*. Kluwer Academic Publishers Group, Boston, 1998
- [41] A. Uhl. Image compression using non–stationary and inhomogeneous multiresolution analyses. *Image and Vision Computing*, 14(5): 365–371, 1996
- [42] A. Uhl. Parallel algorithms for using non–stationary MRA in image compression. In L. Bougne, P. Fraigniaud, A. Mignotte and Y. Robert, editors, *Parallel Processing. Proceedings of EuroPar '96*, volume 1124 of *Lecture Notes on Computer Science*, pages 151–154, Springer, 1996
- [43] A. Uhl. Generalized wavelet decompositions in image compression: arbitrary subbands and parallel algorithms. *Optical Engineering*, 36(5): 1480–1487, 1997
- [44] M. Unser and A. Aldroubi. A review of wavelets in biomedical applications. *Proceedings of the IEEE*, 84(4): 626–638, 1996
- [45] I. Urriza, L. A. Barragan, J. I. Artigas, J. I. Garcia and D. Navarro. Choice of word length in the design of a specialized hardware for lossless wavelet compression of medical images. *Optical Engineering*, 36(11): 3033–3042, November 1997
- [46] J. D. Villasenor, B. Belzer and J. Liao. Filter–evaluation and selection in wavelet image compression. In J. A. Storer and M. A. Cohn, editors, *Proceedings Data Compression Conference DCC '94, Snowbird Utah*, pages 351–360, *IEEE Computer Society*, 1994
- [47] G. K. Wallace. The JPEG still picture compression standard. *Communications of the ACM*, 34(4): 30–44, 1991
- [48] J. Wang and H. K. Huang. Medical image compression by using three–dimensional wavelet transformation. *IEEE Transactions on Medical Imaging*, 15(4), August 1996
- [49] M. V. Wickerhauser. *Adapted wavelet analysis from theory to software*. A. K. Peters, Wellesley, Mass., 1994
- [50] S. Wong, L. Zaremba, D. Gooden and H. K. Huang. Radiologic image compression — a review. *Proceedings of the IEEE*, 83(2): 194–219, 1995
- [51] Z. Xiong, K. Ramchandran and M. T. Orchard. Efficient arithmetic coding for wavelet image compression. In J. Biemond and E. J. Delp, editors, *Visual Communications and Image Processing '97* volume of *SPIE Proceedings*, pages 13–24, San Jose, February 1997

- [52] Z. Xiong, K. Ramchandran and M. T. Orchard. Wavelet packet image coding using space–frequency quantization. *IEEE Transactions on Image Processing*, 7(6): 892–898, June 1998